Energy Dissipation Model for Irregular Breaking Waves

Winyu Rattanapitikon¹ and Tomoya Shibayama²

Abstract

A simple model is presented to compute the average rate of energy dissipation in irregular breaking waves. The average rate of energy dissipation rate is assumed to be proportional to the difference between the local mean energy flux and stable energy flux. The local fraction of breaking waves is determine from the derivation of Battjes and Janssen (1978). Root mean square wave height deformation is computed from the energy flux conservation. The model is validated using root mean square wave height data from small and large scale laboratory and field experiments. Total 144 wave height profiles are used in the calibration and verification of the model. Reasonable good agreement is obtained between the measured and computed root mean square wave heights. The root mean square relative error of the model is 10.2 %.

1. Introduction

In studying many coastal engineering problems it is essential to have accurate information on wave conditions. When waves propagate to the shore, they increase in height and decrease in length wave and eventually waves break. Once the waves start to break, energy flux from offshore is dissipated to turbulence and heat and causes the decreasing of wave height towards the shore in the surf zone. Irregular wave breaking is more complex than regular wave breaking. In contrast to regular waves there is no welldefined breaking point for irregular waves. The highest waves tend to break at greatest distances from the shore. Thus, the energy dissipation of irregular waves occurs over a considerably greater area than that of regular waves.

¹Asst. Prof., Dept. of Civil Engineering, Sirindhorn International Institute of Technology, Thammasat University, Klong Luang, Phatum Thani 12121, Thailand. ²Prof., Dept. of Civil Engineering, Yokohama National University, 79-5 Tokiwadai, Hodogaya-ku, Yokahama 240-8501, Japan. For computing beach transformation, the wave model should be kept as simple as possible because of the frequent updating of wave field for accounting the variability of mean water surface and the change of bottom profiles. In the present study, wave height transformation is computed from the energy flux conservation:

$$\frac{\partial \left(Ec_{g}\cos\theta\right)}{\partial x} = -\overline{D}_{B} \tag{1}$$

where *E* is the wave energy density, c_g is the group velocity, θ is the mean wave angle, *x* is the distance in cross-shore direction, and \overline{D}_B is the average energy dissipation rate of the breaking waves. Snell's law is employed to describe wave refraction.

The wave height transformation can be computed from the energy flux balance equation (Eq. 1) by substituting the formula of the average energy dissipation rate, \overline{D}_{B} , and numerical integrating from offshore to shoreline. The main difficulty of energy flux conservation approach is how to determine the average energy dissipation rate, \overline{D}_{B} . Owing to the complexity of wave breaking mechanism, an empirical approach based on measured data is the only feasible way of describing the energy dissipation rate.

In order to make the empirical formula reliable, it is necessary to calibrate or verify that formula with wide range of experimental results. Since many energy dissipation models were developed based on data with the limited experimental conditions, there is still a need for more data to confirm the underlying assumptions and to make the model more reliable. The main target of this study is to develop the energy dissipation model based on wide range of experimental conditions. Small and large scale laboratory and field experiments have been collected for calibration and verification of the present models. A summary of the collected experimental results is given in Table 1.

Sources	Total No. of cases	Bed condition	Apparatus
SUPERTANK project (Kraus and Smith, 1994)	128	sandy beach	large-scale
Smith and Kraus (1990)	12	plane and barred beach	small-scale
Thornton and Guza (1986)	4	sandy beach	field
Total	144		

The energy dissipation model of irregular breaking wave will be developed based on a similar concept as regular breaking wave model of the authors. The summaries of related regular wave models are as follows.

a) Dally et al. (1985) assumed D_B is proportional to the difference between the local energy flux and the stable energy flux of breaking wave:

$$D_{B} = \frac{K_{d}c_{g}\rho g}{8h} \left[H^{2} - (\Gamma h)^{2}\right]$$
⁽²⁾

where all variables are computed based on linear wave theory, K_d is the wave decay factor (=0.15), H is the local wave height, h is the local water depth, Γ is the stable wave factor (=0.4).

b) Rattanapitikon and Shibayama (1996) modified the model of Dally et al. (1985) and proposed to compute the stable wave factor, Γ :

$$\Gamma = \exp\left[-0.36 - 1.25 \frac{h}{\sqrt{LH}}\right]$$
(3)

where L is the wavelength.

Nine sources of published laboratory results, totally 332 wave profiles, were used to verify the formula.

2. Model Development

Dally (1992) used the regular wave model of Dally et al. (1985) to simulate transformation of irregular wave by using wave-by-wave approach. This means that Dally assumed that D_{b} is proportional to the difference between <u>local energy flux of a breaking wave</u> and stable energy flux. Also wave-by-wave approach requires much computation time. Therefor it may not suitable to use in a beach deformation model.

However, the model becomes simple if we consider the macro-features by set an assumption that the average rate of energy dissipation in irregular breaking waves is proportional to the difference between local mean energy flux and stable energy flux. After incorporating the fraction of breaking, the average rate of energy dissipation in irregular wave breaking, \overline{D}_B , can be expressed as

$$\overline{D}_B = \frac{K_1 Q_b c_g}{h} \left[E_m - E_s \right] \tag{4}$$

where

$$E_m = \frac{1}{8} \rho g H_{max}^2 \tag{5}$$

$$E_{s} = \frac{1}{8} \rho g H_{s}^{2} = \frac{1}{8} \rho g (\Gamma_{ir} h)^{2}$$
(6)

in which all variables are computed based on the linear wave theory, K_1 is the proportional constant, Q_b is the fraction of breaking waves, c_g is the group velocity related to the peak spectral wave period T_p , E_m is the local mean energy density, E_s is the stable energy flux, H_{rms} is the root mean square wave height, H_s is the stable wave height and Γ_{ir} is the stable wave factor of irregular wave.

Rewriting Eq. (4) in term of wave height:

$$\overline{D}_{B} = \frac{K_{1}Q_{b}c_{g}\rho g}{8h} \left[H_{rms}^{2} - (\Gamma_{ir}h)^{2}\right]$$
(7)

The stable wave factor, Γ_{ir} , is determined by applying Eq. (3) as

$$\Gamma_{ir} = \exp\left[K_2(-0.36 - 1.25 \frac{h}{\sqrt{L_p H_{rus}}})\right]$$
(8)

where K_2 is the coefficient, L_p is the wavelength related to the peak spectral wave period.

The local fraction of breaking waves, Q_b , is the ratio of the number of breaking waves to the total number of waves. To determine the fraction of breaking waves, Battjes and Janssen (1978) assumed that the probability density function of wave heights is the Rayleigh-type. The fraction of breaking waves is derive based on the assumption of truncated Rayleigh distribution at the breaking wave height:

$$\frac{1-Q_b}{-\ln Q_b} = \left(\frac{H_{rms}}{H_b}\right)^2 \tag{9}$$

where H_b is the breaking wave height.

Various empirical formulas have been proposed to compute the breaking wave height, e.g., Goda (1970), Weggel (1972), Singamsetti and Wind (1980), and Hansen 1990. However there is no conclusion that which one is the best. Since the breaking criterion of Goda (1970) was developed from wide range of experimental results, it is selected for inclusion into the present model. The breaking criteria of Goda (1970) is

$$H_{b} = K_{3}L_{o}\left\{1 - \exp\left[-1.5\frac{\pi h}{L_{o}}\left(1 + 15m^{4/3}\right)\right]\right\}$$
(10)

where K_3 is the coefficient, L_o is the deep-water wavelength, and *m* is the bottom slope. The published value of K_3 is 0.17 for regular breaking waves. For the present study, K_3 is the adjustable coefficient to allow for effect of the transformation to irregular waves.

Since Eq. (9) is an implicit equation, the iteration process is necessary to compute the fraction of breaking waves, Q_b . It will be more convenient if we can compute Q_b from the explicit form of Eq. (9). From the multi-regression analysis, the explicit form of Q_b can be expressed as the following (with $R^2 = 0.999$):

$$Q_{b} = \begin{cases} 0 & for \frac{H_{rms}}{H_{b}} \le 0.43 \\ -0.738 \left(\frac{H_{rms}}{H_{b}}\right) - 0.280 \left(\frac{H_{rms}}{H_{b}}\right)^{2} + 1.785 \left(\frac{H_{rms}}{H_{b}}\right)^{3} + 0.235 & for \frac{H_{rms}}{H_{b}} > 0.43 \end{cases}$$
(11)

The energy dissipation model (Eqs.7, 8 and 10) contains 3 coefficients, $K_1 - K_3$, that can be found from model calibration.

3. Model Calibration

The model is calibrated for determining the optimal values of the coefficients $K_1 - K_3$ in Eqs. (7), (8) and (10). The calibration is carried out with the large-scale experimental data from the SUPERTANK Laboratory Data Collection Project (Kraus and Smith, 1994). The SUPERTANK project was conducted to investigate cross-shore hydrodynamic and sediment transport processes, during the period August 5 to September 13, 1992, at Oregon State University, Corvallis, Oregon, USA. A 76-m-long sandy beach was constructed in a large wave tank of 104 m long, 3.7 m wide, and 4.6 m deep. Wave conditions involved regular and irregular waves. The 20 major tests werc performed and each major test consisted of several cases (see Table 2). Most of the major tests were performed under the irregular wave actions, except the test No. STBO, STEO, STFO, STGO, STHO, and STIO. The collected experiments for irregular waves include 128 cases of rms wave height profiles, covering incident rms wave heights from 13.9 cm to 60.1 cm, peak wave periods from 2.8 sec to 9.8 sec. Sixteen resistance wave gages were deployed at 3.66 m intervals from the mid surf zone to the wave paddle. Ten capacitance wave gage were placed at 0.61-to 1.83-m intervals in the vicinity of the shoreline and on the beach face to measure runup properties. The measured data from 18 wave gages (16 from resistance wave gage and 2 from capacitance wave gages) are used in this study.

In order to evaluate the accuracy of the prediction, the verification results are presented in term of root mean square (rms) relative error, ER, which is defined as

$$ER = 100 \sqrt{\frac{\sum_{i=1}^{m} (H_{ci} - H_{mi})^2}{\sum_{i=1}^{m} H_{mi}^2}}$$
(12)

where *i* is the wave height number, H_{ci} is the computed wave height of number *i*, H_{mi} is the measured wave height of number *i*, and *tn* is the total number of measured wave height. Smaller values of *ER* correspond to a better prediction.

The *rms* wave height transformation is computed by the numerical integration of energy flux balance equation (Eq. 1) with the energy dissipation rate \overline{D}_B of Eq. (7):

$$\frac{\partial \left(H_{rms}^2 c_g \cos \theta\right)}{\partial x} = -\frac{K_1 Q_b c_g}{h} \left[H_{rms}^2 - \left(h \exp(-0.36K_2 - 1.25K_2 \frac{h}{\sqrt{L_p H_{rms}}})\right)^2 \right]$$
(13)

where Q_b is computed from Eq. (11), and H_b is computed from Eq. (10).

The measured water depth and wave height and wave period at the most seaward wave gage are used as input to the model. Eq. (13) is solved by backward finite difference scheme. Trial simulations indicated that $K_1 = 0.10$, $K_2 = 1.60$, and $K_3 = 0.10$ give good agreement between measured and computed *rms* wave heights. Finally, the energy dissipation rate of irregular wave breaking can be written as

$$\overline{D}_{B} = \frac{0.1Q_{h}c_{g}\rho g}{8h} \left[H_{rms}^{2} - \left(h\exp(-0.58 - 2.00\frac{h}{\sqrt{L_{p}H_{rms}}})\right)^{2} \right]$$
(14)

where Q_h is computed from Eq. (11) and

$$H_{b} = 0.1L_{o} \left\{ 1 - \exp\left[-1.5 \frac{\pi h}{L_{o}} \left(1 + 15m^{4/3} \right) \right] \right\}$$
(15)

Comparison between measured and computed *rms* wave heights for all 128 cases are shown in Fig. 1. Table 2 shows the *rms* relative error, *ER*, of the present model for each major tests. The average *rms* relative error, *ER*, for all 128 cases is 10.0 % which indicates very well prediction. Typical examples of computed *rms* wave height transformation for each major test are shown in Figs. 2 and 3. From Table 2 and Figs. 2-3, it can be seen that the model results generally show very well prediction, except the test no. STKO (broad-crested offshore mound). Furthermore, for some cases, the model tends to under-predict the wave heights very close to the shore.

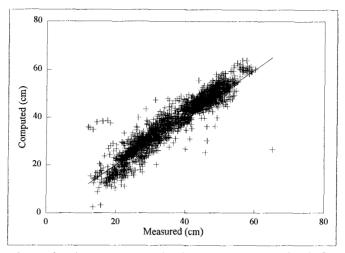


Figure 1 Comparison between computed and measured *rms* wave height for 128 cases of large-scale experiments (measured data from SUPERTANK project).

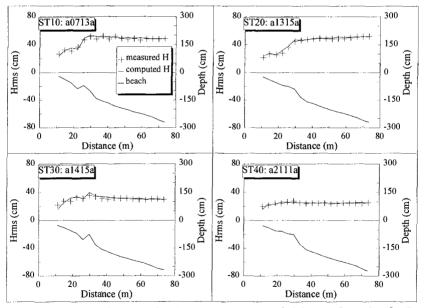


Figure 2 Examples of computed and measured *rms* wave height transformation for Test No. ST10-ST40 (measured data from SUPERTANK project).

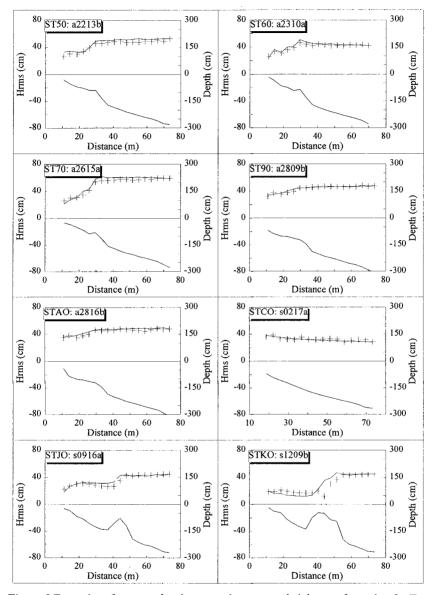


Figure 3 Examples of computed and measured *rms* wave height transformation for Test No. ST50-STKO (measured data from SUPERTANK project).

Table 2. Root mean square relative error (ER) of the present model comparing with
irregular wave data from SUPERTANK project (Kraus and Smith, 1994).

Test	Description	Total	ER. of
No.		No.	Present
		of	study
		cases	
ST10	Erosion toward equilibrium, irregular waves	26	5.82
ST20	Acoustic profiler tests, regular and irregular waves	8	6.96
ST30	Accretion toward equilibrium, irregular waves	19	9.99
ST40	Dedicated hydrodynamics, irregular waves	12	10.28
ST50	Dune erosion, Test 1 of 2, irregular waves	8	12.26
ST60	Dune erosion, Test 2 of 2, irregular waves	9	10.03
ST70	Seawall, Test 1 of 3, irregular waves	9	8.21
ST80	Seawall, Test 2 of 3, irregular waves	3	11.03
ST90	Berm flooding, Test 1 of 2, irregular waves	3	4.99
STAO	Foredune erosion, irregular waves	1	5.83
STBO	Dedicated suspended sediment, regular waves	0	-
STCO	Seawall, Test 3 of 3, irregular waves	8	10.21
STDO	Berm flooding, Test 2 of 2, irregular waves	3	13.96
STEO	Laser Doppler velocimeter, Test 1/2, regular waves	0	-
STFO	Laser Doppler velocimeter, Test 2/2, regular waves	0	-
STGO	Erosion toward equilibrium, regular waves	0	-
STHO	Erosion, transition toward accretion, regular waves	0	-
STIO	Accretion toward equilibrium, regular waves	0	-
STJO	Narrow-crested offshore mound, regular and	10	11.03
	irregular waves		
STKO	Broad-crested offshore mound, regular and irregular	9	23.15
	waves		
	Total	128	9.99

4. Model Verification

Since the present model is calibrated with only the data from the large-scale experiments, there is still a need of data from small-scale and field experiments for confirming ability of the present model. Two sources of experimental results are collected to verify the model, i.e., small-scale experimental data of Smith and Kraus (1990), and field data of Thornton and Guza (1986).

The wave height transformation is computed from the energy flux balance equation (Eq. 1) using \overline{D}_{B} from Eq. (14) and numerical integration, using backward finite difference scheme, from offshore to shoreline. All coefficients in the model are kept to be constant for all cases in the verification.

4.1 Comparison with small-scale laboratory data

The small-scale laboratory data of Smith and Kraus (1990) is used in this subsection. The experiment was conducted to investigate the macro-features of wave breaking over bars and artificial reefs using small wave tank of 45.70-m-long, 0.46-m-wide, and 0.91-m-deep. Submerged triangular-shaped obstacles representing bars and reefs were installed on a 1/30 concrete slope to cause wave breaking. Both regular and irregular waves were employed in this experiment. Total 12 cases were performed for irregular wave tests. Three irregular wave conditions were generated for three bar configurations each, as well as for the control case of plane beach. The wave conditions were developed from input JONSWAP spectrum for spectral peak periods of 1.0, 1.5. and 1.75 sec, with significant wave heights of 11.3, 14.3, and 13.7 cm, respectively. Eight resistance wave gages were installed in the wave tank, 3 gages were placed in the offshore zone, 1 gage was place at the incipient break point, and 4 gages were placed in the surf zone.

Comparison between measured and computed *rms* wave heights for all cases are shown in Fig. 4. The average *rms* relative error, *ER*, for all cases is 11.2 % which indicates a good prediction of the model. Fig. 5 shows the typical examples of computed *rms* wave height transformation for incident *rms* wave height of 10 cm, peak period of 1.75 s and four bottom conditions. The model results generally show good agreement with the measured data. However, the model could not predict the rapid increase and decrease in wave heights near the narrow-crested bar.

4.2 Comparison with field data

The field data from Thornton and Guza (1986) are used in this subsection. The experiment was conducted on a beach with nearly straight and parallel depth contours at Leadbetter Beach, Santa Barbara, California, USA, to measure longshore currents, waves, and beach profiles, during the period January 30 to February 23, 1980.

Comparison between computed and measured rms wave height for all four cases are shown in Fig. 6. The average rms relative error, ER, is 14.5%. Fig. 7 shows the typical examples of computed and measured rms wave height transformation for the cases of Thornton and Guza (1986). The model results also generally show good agreement with the measured data.

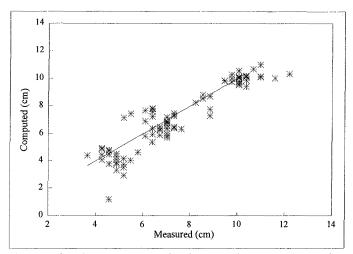


Figure 4 Comparison between computed and measured *rms* wave height for 12 cases of small-scale experiments (measured data from Smith and Kraus, 1990).

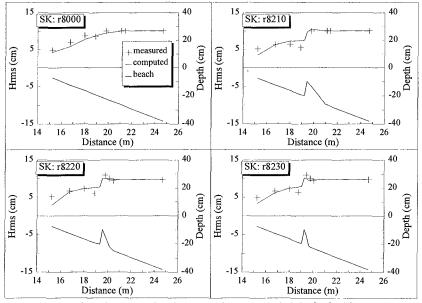


Figure 5 Examples of computed and measured *rms* wave height for incident *rms* wave height of 10 cm, and peak period of 1.75 s (measured data from Smith and Kraus 1990).

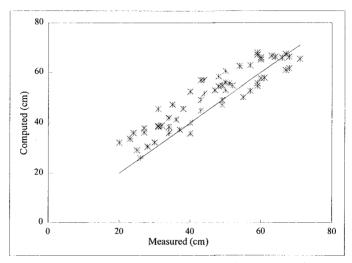


Figure 6 Comparison between computed and measured *rms* wave height for 4 cases of field experiments (measured data from Thornton and Guza, 1986).

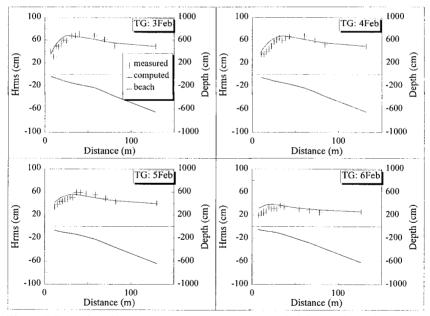


Figure 7 Examples of computed and measured *rms* wave height transformation for cases 3Feb - 6Feb (measured data from Thornton and Guza, 1986).

5. Conclusions

The energy dissipation model for irregular breaking waves is developed and applied to compute *rms* wave heights by using energy flux conservation law. The model is developed based on the modified regular breaking waves model of Dally et al. (1985) and on the local fraction of breaking waves of Battjes and Janssen (1978). The computed *rms* wave heights agreed well with the measured data for general cases, except the case of broad-crested offshore mound which is shown only fairly well prediction. The model is capable of simulating the increase in *rms* wave height due to shoaling and subsequent decrease due to wave breaking over wide range of wave conditions and various shape of beach profiles. The validity of model is confirmed by small scale laboratory data from Smith and Kraus (1990), large scale laboratory data from SUPERTANK project and field data from Thornton and Guza (1986). Table 3 shows the average *rms* relative error, *ER*, of the present model for each data sources. The average *rms* relative error, *ER*, of the model is 10.2 %.

No.	Sources	No. of data sets	No. of data points	<i>ER</i> of Present study
1	SUPERTANK project (Kraus and Smith, 1994)	128	2223	9.99
2	Smith and Kraus (1990)	12	96	11.23
3	Thornton and Guza (1986)	4	60	14.50
	Total	144	2379	10.21

Table 3.	Root mean so	uare relative error	(ER)) of the	present model.
----------	--------------	---------------------	------	----------	----------------

Acknowledgments

This research was sponsored by the Thailand Research Fund. The authors wish to express their gratitude to Prof. Yoshimi Goda of the Yokohama National University for his comments and fruitful discussions. Thanks and sincere appreciation are expressed to Dr. Nicholas C. Kraus, Dr. Jane McKee Smith, Dr. Edward B. Thornton and Dr. R.T. Guza for providing the experimental data used in this work.

References

Battjes, J. A., and Janssen, J.P.E.M. (1978). Energy loss and set-up due to breaking of random waves, Proc. 16th Coastal Engineering Conf., ASCE, pp. 569-587.

Dally, W.R., Dean, R.G., and Dalrymple, R.A. (1985). Wave height variation across beach of arbitrary profile, J. of Geo. Res., Vol. 90, No. C6, pp. 11917-11927.

Dally, W.R. (1992). Random breaking waves: Field verification of a wave-by-wave algorithm for engineering application, Coastal Engineering, Vol. 16, pp. 369-397.

Goda, Y. (1970). A synthesis of breaking indices, Trans. Japan Soc. Civil Eng., Vol. 2, Part 2, pp. 227-230.

Hansen, J.B. (1990). Periodic waves in the surf zone: Analysis of experimental data, Coastal Engineering, Vol. 14, pp. 19-41.

Kraus, N.C., and Smith, J.M. (1994). SUPERTANK Laboratory Data Collection Project, Technical Report CERC-94-3, U.S. Army Corps of Engineers, Waterways Experiment Station, Vol. 1-2.

Rattanapitikon, W. and Shibayama, T. (1996), Cross-shore sediment transport and beach deformation model, Proc. 25th Coastal Eng. Conf., ASCE, pp. 3062-3075.

Singamsetti, S.R. and Wind, H.G. (1980), Breaking waves: Characteristics of shoaling and breaking periodic waves normally incident to plane beaches of constant slope, Delf Hydraulic Lab., Rep. M1371, 142 pp.

Smith, J.M. and Kraus, N.C., (1990). Laboratory study on macro-features of wave breaking over bars and artificial reefs, Technical Report CERC-90-12, U.S. Army Corps of Engineers, Waterways Experiment Station.

Thornton, E.B. and Guza, R.T. (1986). Surf zone longshore currents and random waves: field data and model, J. of Physical Oceanography, Vol. 16, pp. 1165-1178.

Weggel, R.J. (1972). Maximum breaker height, J. of the waterways, Harbors, and Coastal Engineering Division, Vol. 98, No. ww4, pp. 529-548.